Title

The effect of STAT3 inhibition on status epilepticus and subsequent spontaneous seizures in the pilocarpine model of acquired epilepsy.

Authors

Grabenstatter, HL
Del Angel, Y Cruz
Carlsen, J
et al.

Publication Date

2014-02-01

DOI

10.1016/j.nbd.2013.09.003

Peer reviewed

Published in final edited form as:
Neurobiol Dis. 2014 February ; 62: 73–85. doi:10.1016/j.nbd.2013.09.003.

The effect of STAT3 Inhibition on status epilepticus and subsequent spontaneous seizures in the Pilocarpine Model of Acquired Epilepsy

H. L. Grabenstatter[a,†], **Y. Cruz Del Angel**[a,†], **J. Carlsen**[a], **M. F. Wempe**[b], **A. M. White**[a], **M. Cogswell**[c], **S. J. Russek**[c], and **A. R. Brooks-Kayal**[a,b,d,e,*]

[a]Department of Pediatrics, Division of Neurology, and the Translational Epilepsy Research Program, University of Colorado School of Medicine, Aurora, CO

[b]Department of Pharmaceutical Sciences, Skaggs School of Pharmacy and Pharmaceutical Sciences, University of Colorado Anschutz Medical Campus, Aurora, CO

[c]Department of Pharmacology and Experimental Therapeutics, Boston University School of Medicine, Boston, MA

[d]Department of Neurology, University of Colorado School of Medicine, Aurora, CO

[e]Children's Hospital Colorado, Aurora, CO

Abstract

Pilocarpine-induced status epilepticus (SE), which results in temporal lobe epilepsy (TLE) in rodents, activates the JAK/STAT pathway. In the current study, we evaluate whether brief exposure to a selective inhibitor of the JAK/STAT pathway (WP1066) early after the onset of SE effects the severity of SE or reduces later spontaneous seizure frequency via inhibition of STAT3-regulated gene transcription. Rats that received systemic WP1066 or vehicle at the onset of SE were continuously video-EEG monitored during SE and for one month to assess seizure frequency over time. Protein and/or mRNA levels for pSTAT3, and STAT3-regulated genes including: ICER, *Gabra1*, c-myc, mcl-1, cyclin D1, and bcl-xl were evaluated in WP1066 and vehicle-treated rats during stages of epileptogenesis to determine the acute effects of WP1066 administration on SE and chronic epilepsy. WP1066 (two 50 mg/kg doses) administered within the first hour after onset of SE results in transient inhibition of pSTAT3 and long-term reduction in spontaneous seizure frequency WP1066 alters the severity of chronic epilepsy without affecting SE or cell death. Early WP1066 administration reduces known downstream targets of STAT3 transcription 24 hours after SE including cyclin D1 and mcl-1 levels, known for their roles in cell-cycle progression and cell survival, respectively. These findings uncover a potential effect of the JAK/STAT pathway after brain injury that is physiologically important and may provide a new therapeutic target that can be harnessed for the prevention of epilepsy development and/or progression.

[*]To whom correspondence should be addressed: Amy Brooks-Kayal, Department of Pediatrics, Division of Neurology, University of Colorado School of Medicine and Children's Hospital of Colorado, amy.brooks-kayal@childrenscolorado.org.
[†]These authors contributed equally to experimental design and data acquisition.

Introduction

Epilepsy is one of the most common neurological disorders in humans, and afflicts more than 1% of the population and 65 million people worldwide (England et al., 2012). The most common form of acquired epilepsy is temporal lobe epilepsy (TLE), and over 30% of patients with TLE have seizures that are refractory to commonly used anticonvulsant drugs (Bauer and Burr, 2002). A subset of patients with TLE clearly demonstrate progressive and more severe epilepsy over months to years after the onset of epilepsy (Berg et al., 2003). All currently marketed anticonvulsants symptomatically treat seizures, and there are currently no approved medications that are capable of modifying the disease to lessen the severity of the underlying epilepsy and the associated co-morbidities.

Epileptogenesis refers to all of the anatomical, biochemical, and physiological processes occurring in brain that lead to the emergence of spontaneous network hypersynchronicity, seizures, and epilepsy. TLE is often an injury-induced or lesion-associated, acquired condition characterized by a period ranging from days or weeks (in rodents) to months or years (in humans) after a brain insult before the onset of spontaneous seizures (early epileptogenesis). Epilepsy onset may be followed by a progressive increase in frequency and severity of seizures (late epileptogenesis). In an animal model of acquired epilepsy, continuous video-EEG monitoring was used to determine whether inhibition of JAK/STAT pathway activation at the time of brain insult (status epilepticus; SE) using an inhibitor of STAT3 phosphorylation (WP1066) would alter status epilepticus, prevent the development of spontaneous seizures, or alter the severity of chronic epilepsy (i.e., increased seizure frequency over time).

The JAK/STAT pathway is composed of 4 JAK proteins (JAK1, 2, 3, and TYK) and 7 STAT proteins (STAT 1, 2, 3, 4, 5A, 5B, and 6) in mammals (Aaronson et al., 2002). The majority of these proteins are inactive in the cytoplasm until membrane-bound receptors are bound by a variety of extracellular signaling proteins (e.g., Il-6, gp-130, PDGF, FGF, BDNF) to initiate the signal transduction cascade. JAKs are consequently recruited to the membrane where they are phosphorylated by the integral receptor kinases, and are activated to recruit and phosphorylate target STAT proteins (Darnell et al., 1994; Zhong et al., 1994a, Zhong et al., 1994b; Schindler et al., 1995; Ihle et al., 1996). Phosphorylated STAT proteins (pSTATs) dimerize and translocate to the nucleus where they bind specific STAT DNA regulatory elements in the promoters of target genes to alter their transcription (Aaronson et al., 2002; Zhong et al., 1994a, Zhong et al., 1994b, Levy et al., 2002). The JAK/STAT pathway is dynamically controlled at many levels by phosphorylation, nuclear trafficking, and dimerization.

While several physiological roles for JAK/STAT proteins have been characterized outside of the brain, recent evidence suggests that this pathway is activated after a variety of brain insults that can lead to epilepsy. Activation of this pathway has been demonstrated after both pilocarpine and kainate-induced SE (Lund et al., 2008, Xu et al., 2011, Choi et al., 2003), after traumatic brain injury (TBI [Oliva et al., 2011; Zhao et al., 2011; Raible et al., 2012]), and after ischemia (Planas et al., 1996; Suzuki et al., 2001). The transcription factor STAT3 is known to have important roles in regulating gene expression, specifically increasing genes important to cell survival (e.g., mcl-1, bcl-2, bcl-xl), cell proliferation (e.g., c-myc), cell-cycle progression (e.g., cyclin D1), and angiogenesis (e.g., VEGF), both during normal development and in epileptogenesis. Activation of the JAK/STAT signaling cascade, and specifically phosphorylation of STAT3, also drives ICER transcription after SE (Lund et al., 2008). Interestingly, the transcriptional repression of *Gabra1* following pilocarpine-induced SE and in acute primary neuronal culture is mediated by ICER and phosphorylated CREB (Lund et al., 2008; Hu et al., 2008). Thus, the current experiments aimed to further elucidate

the role of early JAK/STAT pathway activation in the development and progression of epilepsy, specifically whether brief inhibition of STAT3 phosphorylation affects the severity of SE or reduces the frequency of later spontaneous seizures.

Material and Methods

WP1066

Several small molecule inhibitors of pSTAT3 have been created to interfere with the signaling of STAT3, including blockade of the ligand-receptor interaction and the activation sites of STAT3, pSTAT3 dimerization, nuclear translocation of pSTAT3, pSTAT3 DNA binding, and subsequent gene transcription. The STAT3 inhibitor AG490 has been studied extensively, but it has a relatively low potency (IC50 >50μM *in vitro*) and lack of biostability prevents its use *in vivo*. Thus, WP1066 (named for Waldemer Priebe) was developed from a series of small molecule STAT3 inhibitors designed from the caffeic acid benzyl ester/AG490 scaffold (Kupferman et al., 2009; Iwamaru et al., 2007; Hussain et al., 2007) to optimally inhibit the JAK2/STAT3 interaction and subsequent phosphorylation of STAT3 at tyrosine 705 (Ferrajoli et al., 2007).

WP1066 (EMD Biosciences, San Diego, CA) is a cell-permeable AG490 tyrphostin analog that acts as an effective STAT3 pathway inhibitor (Kupferman et al., 2009; Iwamaru et al., 2007; Hussain et al., 2007) and is a potent antitumor agent that inhibits malignant glioma growth both in cultures *in vitro* and in mice *in vivo* (Iwamaru et al., 2007). WP1066 crosses the blood-brain barrier and achieves therapeutic CNS concentrations after intraperitoneal (i.p.) administration in rodent models of CNS tumors (Iwamaru et al., 2007; Hussain et al., 2007).

Bio-Analytical Pharmacokinetic (BAPK) Analysis

Rat Liver Microsomal Incubations—Rat liver microsomal incubations were performed as follows: (i) a mixture of PBS (50 mM; pH 7.4), $MgCl_2$ (5.0 mM), UDPGA (4.0 mM, cofactor for glucuronidation; *e.g.* UGTs), NADPH (1.0 mM, cofactor for monooxygenases, *e.g.*, cytochrome P450, [Sigma-Adrich, St. Louis, MO]), 1.0 μM WP1066 (DMSO ≤ 0.01%, total v/v), and 20 mg/ml liver microsomal protein (Xenotech LLC, Lenexa, KS) were pre-incubated at 37.0 ± 0.1 °C; (ii) incubations were initiated by test compound addition and mixing (1.0 μM final). After initiation (0.5 min), and at 5, 10, 15, 30 and 60 min, incubated samples were removed and added to quench solution (cold acetonitrile, Fischer Scientific, Pittsburg, PA). The resulting samples were mixed and immediately analyzed by LC/MS-MS.

An Applied Biosystems Sciex 4000 ® (Applied Biosystems; Foster City, CA) equipped with a Shimadzu HPLC (Shimadzu Scientific Instruments, Inc.; Columbia, MD) and Leap auto-sampler (LEAP Technologies; Carrboro, NC) was used. Compared to the negative ion mode, WP1066 displayed enhanced analytical sensitivity (data not shown) via electrospray ionization positive ion mode (ESI +). Consequently, the following liquid-chromatography mass spectrometry conditions were used: i) an ion-spray voltage of 5000 V; ii) temperature, 450 °C; iii) curtain gas (CUR; set at 10) and Collisionally Activated Dissociation (CAD; set at 5) gas were nitrogen; iv) Ion Source gas one (GS1) and two (GS2) were set at 30; v) entrance potential was set at 10.0 V; vi) quadruple one (Q1) and (Q3) were set on Unit resolution; vii) dwell time was set at 200 msec; and viii) declustering potential (DP), collision energy (CE), and collision cell exit potential (CXP) are voltages (V). Compound settings were 356.0 → 105.1 *m/z*, DP = 60, CE = 31, CXP = 6. Liquid chromatography employed an Agilent Technologies, Zorbax extended-C18 50 x 4.6 mm, 5 micron column with a column guard at 40 °C with a flow-rate of 0.4 mL/min. The mobile phase consisted of

A: 10 mM ammonium acetate, 0.1% formic acid in water, and B: 50:50 ACN:MeOH. Between samples the auto sampler was washed with a 1:1:1:1 mixture of ACN:MeOH:IPA:water. The chromatography method used was 95% A for 1.00 min; ramped to 95% B at 3.00 min and held for 4.50 min; next, brought back to 95% A at 8.50 min and held for 1.00 min (9.5 min total run time). WP1066 had a retention time of 4.2 min.

Isolation of the plasma and tissue for pharmacokinetic analysis—At specific time points relative to WP1066 administration, ~500 μl whole blood was collected into ice-cold EDTA-coated tubes (Becton Dickinson and Company, Franklin Lakes, NJ). From these samples, plasma (~200 μl) was collected into Eppendorf tubes after centrifugation (14,000 rpm at 4°C for 10 min) and placed onto dry ice. In parallel, the brain, kidneys, and liver, were rapidly removed, flash frozen on dry ice and all samples were stored at −80 ± 10 °C for later pharmacokinetic analyses.

Tissue Homogenates and standard curves—Individual, frozen samples were homogenized (2 min) with two weight volumes of phosphate buffer (PBS; 100 mM, pH 7.4). Standard curve (SC) solutions (10 μL) were prepared and thoroughly mixed with control plasma, blood (Bioreclamation LLC, Liverpool, NY) or homogenate (990 μL) and immediately frozen (−80 ± 10 °C). SC were extracted and processed in an analogous fashion as the *in vivo* samples. Homogenates were sampled in triplicate (125 μL) and extracted with extraction solution (250 μL; 4:1; water: 1:1 ACN:MeOH, Fischer Scientific, Pittsburg, PA). The tubes were vortex mixed and centrifuged at 13,000 rpm for 10 min. The supernatants were transferred into individual wells of a 96-well plate and immediately analyzed via LC/MS-MS. The 96-well plate was placed into the LEAP auto-sampler cool-stack (7.0 ± 1.0 °C). For plasma, blood, and tissue homogenate (kidney, cortex and liver), nine point standard curves (n = 4 ± SD) representing concentrations between 1 – 1200 ng/mL were prepared. All standard curve data were fitted to a $1/x^2$ weighted linear regression; these standard curves were used to determine apparent drug concentrations from the extracted samples.

Pilocarpine-induced SE and WP1066 administration—SE was induced in adult Sprague-Dawley rats (Charles-River Labs, Kingston, PA) using 385 mg/kg i.p. pilocarpine and rats were pre-treated with 1mg/kg i.p. scopolamine to block peripheral cholinergic effects. Control rats received a subconvulsive dose of pilocarpine (38.5 mg/kg i.p.). To decrease the mortality, pilocarpine treated rats received diazepam 6 mg/kg i.p. after 1 hr of SE, and then 3 mg/kg every 2 hrs if needed due to persistent seizures. Control rats received one tenth of the dose of diazepam (0.6 mg/kg). For all treatment studies, WP1066 (50 mg/kg in DMSO) was administered i.p. at onset of SE (defined as the first Class 5 motor seizure) and a second 50 mg/kg WP1066 dose was injected 45 minutes later. Motor seizures were scored by standard behavioral classes (Racine, 1972) as follows: (1) behavioral arrest, eye closure, vibrissae twitching, sniffing: (2) facial clonus and head bobbing; (3) forelimb clonus; (4) rearing with continued forelimb clonus; and (5) rearing with loss of motor control and falling. Pilocarpine was purchased from Sigma (St. Louis, MO), diazepam was purchased from Hospira (Lake Forest, IL) and WP1066 was purchased from EMD Biosciences (San Diego, CA). For all experimental procedures, the animals' care was in accordance with institutional guidelines.

EEG Acquisition and analysis

To accurately analyze electrographic seizure frequency, two bilateral subdural stainless steel screws (4.0 mm posterior, 2.5 mm lateral relative to bregma) were placed over the temporolimbic cortices. Additional stainless steel screws were placed on each side of the brain behind lambda (i.e., over the cerebellum) and were used as reference and ground

electrodes. Animals were allowed to recover from surgery for 1 week before proceeding with any further experimentation. Epileptic rats were video-EEG monitored 24 hours/day using Stellate and Pinnacle digital video-EEG systems. Rats were placed in the recording chamber and flexible cables were attached to a commutator (i.e., electric swivel) system that allows the animal to move freely. EEG signals were sampled at 1 kHz, amplified by 500x, and band-pass filtered between 0.3 Hz and 600 Hz.

Off-line data analyses were performed by trained technicians blinded to all experimental parameters to (1) identify electrographic seizures and (2) analyze indices of electrographic SE after WP1066 and vehicle treatment. Electrographic seizures were differentiated from background noise by the appearance of large-amplitude (at least three times baseline), high frequency (minimum of 5 Hz) activity, with progression of the spike frequency that lasts for a minimum of 10 sec. Electrographic seizures were manually detected in EEG recordings and correlated with behavioral manifestations in continuous video recordings utilizing a modified Racine scale (described above). Electrographic seizures class 3 and above were classified as convulsive and seizures scored as class 2 and below were classified as non-convulsive.

The power analysis was performed using a Fast Fourier Transform (FFT) algorithm written using subroutines in Visual Basic. For the initial analyses, contiguous epochs containing 8192 points (8.192 seconds) each were used. A rectangular window was used. Parameters determined were maximum power, integrated power and time that elapsed from maximum power until within 20%, 10%, and 5% of the baseline power. Compressed spectral analyses (CSA) were also generated for each rat using FFT giving the magnitude of power in each frequency bin. Each pixel in the x direction represents approximately 32 seconds.

For the short-term analyses, rectangular windows of 131072 points (131 seconds) were used. The power in each frequency band (1–4 Hz, 4–8 Hz, 8–13 Hz, 13–30 Hz, 30–50 Hz, and 50–70 Hz) was averaged for 0.5 h, 1 h, 2 h, 4 h, and 6 h-long bins following onset of status and injection of vehicle or drug. This was done for both EEG data channels.

RT-PCR and Western Blots

Rats were anesthetized with inhaled isoflurane, decapitated, and whole brains were dissected in chilled 1X PBS medium (with 1:1000 phosphatase inhibitors) for dentate gyrus microdissection. Longitudinal hippocampal slices (500 μm thick) were cut and the dentate gyrus was identified and dissected under an anatomical microscope. Alternate slices from each hippocampus were used for mRNA and protein extraction to control for any difference in the amount of damage and/or seizure activity in one hippocampus compared to the other. The dentate gyrus was chosen because it has demonstrated changes in pSTAT3, ICER, GABARα1 levels in previous studies (Lund et al., 2008) and is relatively well preserved during epileptogenesis.

For western blots, protein (20–30 μg) extracted from microdissected DG was loaded into 10% (for GABAR subunit) or 8% (for pSTAT3) SDS–polyacrylamide gels and run for ~1.5 h at 115 V. Blots were then transferred to nitrocellulose membranes and blocked in 5% milk/trisbuffered saline with Tween-20 (TBS-T) 1 h at room temperature. Membranes were incubated with rabbit polyclonal antibodies raised against STAT3 phosphorylated at Tyr705 (anti-pSTAT3, Cell Signaling Technologies; 1:1,000), total STAT3 (anti-STAT3, Cell Signaling Technologies; 1:2,000), or GABARα1 (anti- GABARα1 alpha1, Millipore 06-868; 1:5,000) overnight at 4°C in 5% bovine serum albumin/TBS-T (for pSTAT3 or total STAT3) or in 1% milk/TBS-T (for GABAR subunits), Membranes were then washed and incubated with anti-rabbit secondary antibody (GE health, 1:10,000 in 1% milk/TBST) conjugated to horseradish peroxidase for 1 h at room temperature.

Protein bands were detected with the use of chemiluminescent solution (Pierce). Membranes were stripped and probed with rabbit polyclonal antibody raised against β-actin (1:40,000, Sigma) in 1% milk/TBS-T overnight. GABARα1 values were normalized to β-actin expression in the same samples to control for loading amount variability and then expressed as percent change with respect to mean control values in the same run (defined as 1). Phosphorylated STAT3 was normalized to total STAT3 expression and expressed as percent change relative to normalized values for tissue from animals treated with vehicle at SE onset (expressed as 100%) to evaluate any potential effect of WP1066. Densitometry was performed with NIH Image J version 1.42q. Statistical significance was defined as a P value of less than 0.05 and was calculated with Prism software using a One-way ANOVA with a Tukey's test for multiple comparisons or an unpaired student's t-test as indicated.

For ICER RT-PCR, RNA was extracted from microdissected hippocampal DG tissue 6 h after SE using RNeasy Mini RNA extraction kit (Qiagen). Reactions for ICER mRNA (specific primers and probe Rn00569145_m1, Applied Biosystems) were multiplexed with cyclophilin specific primers and probe (Ppia, Rn00690933_m1, Applied Biosystems). Reactions were performed using the ABI Prism 7900HT machine. Samples were repeated in duplicate with each reaction split into two wells in a total volume of 20 μl containing 16ng of RNA. PCR cycling parameters were 50°C for 30 minutes, 95°C for 10 minutes, 50 cycles of 95°C for 15 sec, and 60°C for 1 minute. All values were normalized to control cyclophilin expression for loading variability and then expressed as fold change with respect to the mean control values (defined as 1).

For analysis of STAT3-target genes, RNA was extracted from microdissected DG 24 h after SE using the Trizol reagent protocol (Invitrogen, Carlsbad, CA). To synthesize complementary DNA (cDNA), 0.5–1 μg of RNA was separated and processed with the SuperScript II reverse transcription kit (Invitrogen) according to the manufacturer's instructions and then diluted 1:4 for storage and subsequent RT-PCR. For RT-PCR reactions, each sample was run in triplicate and each 25-μl reaction contained 1.25 μl Taqman primer and probe set for gene of interest (ICER: Rn00569145_m1 (CREM), c-myc: Rn00561507_m1, cyclin D1: Rn00432360_m1, bcl-2: Rn99999125_m1, bcl-xl: Bcl-xl: Rn00437783_m1, mcl-1: Rn00821024_g1, and VEGF: Rn01511601_m1, all Applied Biosystems) or 1.25 μl Taqman Ppia (cyclophilin) primer and probe set (Rn00690933_m1, Applied Biosystems) and 12.5 μl Taqman Universal Master mix, 5 μl of sample cDNA, and 6.25 ml of DEPC water to complete the reaction. RT-PCR was performed on the SDS-7500 PCR machine (Applied Biosystems). The RT-PCR runs consisted of first 1 cycle of 50°C for 2 min, then 1 cycle of 95°C for 10min, and 40 cycles of 95°C for 15 s and 60°C for 1 min. All values were normalized to control cyclophilin expression for loading variability and then expressed as fold change with respect to the mean control values (defined as 1).

Fluoro-Jade B staining

Rats were sacrificed 48 h following onset SE and administration of either WP1066 (50 mg/kg at SE onset and 50 mg/kg 45 min later) or vehicle, perfused transcardially with cold phosphate buffered saline (0.01 M) and 4% paraformaldehyde (in 0.1 M), postfixed overnight, then cryoprotected in 30% sucrose. Frozen, embedded (in Tissue-Tek OCT compound, Sakura Finetek, Torrance, CA) whole brains were serial sectioned in the coronal plane. Mounted coronal brain sections (12μm) were stained with Fluoro-Jade (Histochem, Jefferson, AR), an anionic fluorochrome, to selectively stain degenerating neurons (Schmued and Hopkins, 2000a; Schmued and Hopkins, 2000b). This is a simple, reliable and sensitive technique to detect dying neurons. A 1-in-20 series of sections (i.e., −2.3 mm to −4.8 mm from Bregma) from each brain (e.g., ~20 sections per animal, SE+WP1066, n=9; SE+DMSO, n=11) was processed. The sections were immersed in 100% ethanol for 10 min, followed by 2 min in 70% ethanol, 1 min in distilled water, 2 min in 70% ethanol, and

2 min in distilled water. Slides were transferred to 0.06% potassium permanganate for 10–15 minutes. After a 2-minute rinse with distilled water, sections were placed in Fluoro-Jade staining solution for 10 minutes at room temperature. Following staining, the sections were rinsed three times with distilled water. The slides were dried and immersed in CitriSolv (Fisher, Pittsburgh, PA). Sections were examined under a fluorescence microscope using fluorescein isothiocyanate (FITC) filter sets. Neurons were morphologically identified by size and cytological characteristics, and glial cells were excluded from counts. Fluoro-Jade B positive neuronal cell bodies were counted in the CA1, CA3, and hilar region of the hippocampus using NIS-Elements Analysis software. The selected areas of interest used to quantify Fluoro-Jade B cell density were the same for each section examined. Images were obtained using a 10X objective (Nikon Eclipse TE2000-U). The technician conducting cell counts was blind to treatment administered. Statistical differences between treatments were determined using a Mann-Whitney test.

Neu-N immunoflourescence

Rats were sacrificed >30 days following pilocarpine-induced SE and administration of either WP1066 (50 mg/kg at SE onset and 50 mg/kg 45 min later) or vehicle and following the onset of spontaneous seizures. Rats were perfused, brains were removed to be postfixed overnight and cryoprotected as described above. Frozen, embedded whole brains were serial sectioned in the coronal plane along the rostral-caudal axis as described above and a 1-in-20 series of sections (i.e., −2.3 mm to −4.8 mm from Bregma) from each brain (e.g., ~20 sections per animal; CTRL, n=4; SE+DMSO, n=4, SE+WP1066, n=4) was processed. Dry, mounted slides were washed (in 1X TBS) and blocked, then incubated overnight in mouse anti-NeuN primary antibody (1:1000; in 1X TBS with 0.3% Triton X-100, 10% NGS, 3%BSA, and 1% glycine). Slides were washed (in 1X TBS with 0.3% Triton), then incubated in secondary antibody (1:1000; Alexa 546 goat anti-mouse (A11003, Invitrogen) in 1X TBS with 0.3% Triton X-100, 10% NGS, 3%BSA, and 1% glycine) for 2 h. Slides were washed twice in 1X TBS with 0.3% Triton X-100 and two more times (in 1 X TBS) before viewing with TRITC filter settings and conducting neuronal cell counting as described above.

Results

Pharmacokinetic profile of WP1066

WP1066 was developed as a cancer therapeutic and the compound has not been optimized for use in CNS disorders. Thus, evaluation of the absorption, metabolism and distribution (including blood-brain permeability) of the compound was required prior to initiating long-term *in vivo* testing and to determine an appropriate dosing regime to block early activation of STAT3 following pilocarpine-induced SE. *In vitro* and *in vivo* experiments demonstrate that 100 mg/kg WP1066 has an apparent *in vitro* rat (Sprague-Dawley) plasma half-life (37 °C) of ~1.0 hr (Fig 1A). *In vitro* rat liver microsome data suggest 100 mg/kg WP1066 has moderate stability (Fig 1B). Additionally, cortical concentrations of WP1066 are measurable in rats after i.p. administration of 100 mg/kg WP1066 suggesting some blood-brain barrier permeability. However, these concentrations are only maintained for 5 min after administration and are completely cleared within 15 min (Fig 1C). Additional experiments were conducted with repeated dosing, with 50 mg/kg WP1066 administered at onset of SE and a second 50 mg/kg dose administered 45 minutes later. Samples of cortex, plasma, kidney, and liver were harvested 1 h after the onset of SE. While a complete pharmacokinetic time-course was not performed, low levels of WP1066 were observed in brain tissue (5.8 ± 1.1 ng/g) and in plasma (37.4 ± 13.4 ng/ml) with higher kidney (98.1 ± 33.0 ng/g) and liver (364.9 ± 72.9 ng/g) concentrations, suggesting that the compound can cross the blood-brain-barrier, but metabolism and clearance is very fast (Fig 1D).

JAK/STAT inhibition by WP1066

Brain injuries like SE that lead to subsequent epilepsy development activate the JAK/STAT pathway, and blocking activation of this pathway can prevent the transcription of STAT3-target genes, which may be important to later epilepsy development (Lund et al., 2008). WP1066 administered at the onset of SE (50 mg/kg i.p. in DMSO) and again 45 minutes later, effectively reduces STAT3 phosphorylation in the dentate gyrus (DG) of the hippocampus by 58% 1 h after SE onset (Fig 2A). The effect of the inhibitor is transient, however, as demonstrated by the lack of pSTAT3 inhibition in WP1066-treated animals 6 h after SE onset (Fig 2B). Thus, peripheral administration of WP1066 effectively inhibits early activation of STAT3 phosphorylation during an acute period following SE onset that has been previously associated with increased expression of STAT3 target genes following SE (e.g., ICER [Lund et al., 2008]).

Early treatment with WP1066 does not alter electrographic SE

Our experiments were designed to determine whether WP1066 administered after onset of pilocarpine-induced SE was disease modifying (i.e., prevents the development of epilepsy or reduces the severity of chronic epilepsy). As WP1066 was administered while SE was ongoing, any effects of treatment on severity or duration of SE that could contribute to disease modifying effects needed to be determined. To examine if WP1066 administration altered severity of SE, rats receiving either vehicle or WP1066 (50 mg/kg at SE onset and 50 mg/kg 45 minutes later) were EEG-monitored during and for 48 h after SE. A simple analysis of the magnitude of pilocarpine-induced SE revealed that WP1066 treatment failed to alter any of the initial electrographic parameters measured during SE. Specifically, power present in the 0–50 Hz bandwidth during the first ~19 h following SE was not different in WP1066 and vehicle-treated rats (Fig 3A). Similarly, no significant differences in integrated power over the first 12 h or 24 h after SE onset were observed between vehicle-treated and WP1066-treated rats suggesting the progression of SE was not altered by early JAK/STAT inhibition (Fig 3B). Duration of SE and intensity of SE were also unchanged by WP1066 treatment, as shown by the absence of differences in WP1066-treated rats relative to vehicle-treated rats in measures of integrated power, maximum power, and degradation of maximum power to 20%, 10%, and 5% from the measured maximum (Fig 3C–E). These data suggest that WP1066 administered at onset of SE acutely inhibits activation of the JAK/STAT pathway during the initial stages of epileptogenesis, but does not alter the severity, magnitude, or duration of SE utilizing a simple, quantitative analysis of SE. However, the effect of WP1066 on STAT3 phosphorylation is relatively transient and discrete effects of the drug on specific bandwidths or at acute time points could potentially be masked utilizing the analysis of power within the 0–50 Hz bandwidth for the first 48 h following SE. Therefore, multiple time points (i.e., 30 min, 1 h, 2 h, 4 h, and 6 h) and power in multiple bandwidths (0–4 Hz, 4–8 Hz, 8–13 Hz, 13–30 Hz, 30–50 Hz, and 50–70 Hz) following injection of vehicle or WP1066 were also analyzed to determine if early JAK/STAT inhibition altered SE (Fig 4A–G). No significant differences were observed in integrated power demonstrated in the delta (0–4 Hz), theta (4–8 Hz), alpha (8–13 Hz), beta/gamma (13–30 Hz), 30–50 Hz, 50–70 Hz, or 70–100 Hz bandwidths within 30 min, 1 h, 2 h, 4 h, or 6 h epochs after WP1066 or vehicle administration suggesting early JAK/STAT inhibition does not alter the induction of SE or severity of ongoing SE. Raw traces (0.3 Hz–600 Hz) from WP1066-treated rats relative to vehicle-treated rats (Fig G1a-6a and G1b-6b) at specific time points following administration of WP1066 or vehicle demonstrate no distinguishable treatment-induced difference in the progression of early electrographic SE (i.e., at 30 min, 1 h, 2 h, 4 h, or 6 h).

WP1066 reduces the severity of chronic epilepsy

Overall, seizure frequencies often progressively increase over time in chemoconvulsant-induced animal models of TLE, although in some models this increase is overlaid on a cyclic pattern with periods of increasing and decreasing seizure frequencies over time (often referred to as “clustering” (Williams et al., 2009; Pitkanen, 2007). Similarly, a subset of patients with TLE experience a progressive worsening of their epilepsy, with an increases in seizure frequency, severity, and/or clustering over time from disease onset (Berg et al., 2003; Blume, 2006; Shukla and Prasad, 2012; Balish et al., 1991; Haut et al., 2002; Haut, 2006). WP1066 treatment after onset of SE did not prevent the development of electrographic spontaneous seizures in the pilocarpine model (Fig 5A), and the latency to first spontaneous seizure was similar for WP1066-treated and vehicle-treated rats. However, rats treated with WP1066 exhibit lower daily seizure frequencies (i.e., electrographic seizures per day) across the first 2 weeks following SE relative to vehicle-treated rats, suggesting WP1066 inhibits the progression of early epileptogenesis (Fig 5B). The seizure frequencies for WP1066-treated rats remained relatively unchanged during the first 4 weeks of epileptogenesis, and WP1066-treated rats also had significantly lower daily seizure frequencies relative to vehicle-treated rats during week 4. Although WP1066-treated rats had lower daily seizure frequencies during week 3 compared to vehicle-treated rats, the difference was not significant, likely due to the inter- and intra-animal variability observed in mean daily seizure frequencies over time in the pilocarpine model of rat TLE (Fig 5C). These findings suggest that WP1066 treatment inhibits progressive increases in seizure frequency relative to vehicle-treated animals. The ratio of non-convulsive seizures to convulsive seizures in WP1066-treated rats relative to vehicle-treated rats over the 4-week monitoring period was analyzed to evaluate WP1066 treatment on severity of spontaneous seizures. Rats were only included in this study if they were continuously monitored for the entire 4 weeks. Vehicle-treated rats demonstrated a higher proportion of convulsive seizures relative to nonconvulsive seizures when compared to WP1066-treated rats (Fig 5D). Electrographic spontaneous seizure morphologies were not easily distinguishable based on treatment group and there was no significant difference in seizure duration. Thus, the primary disease modifying effect observed in WP1066-treated rats were (1) inhibition of the progression of seizure frequency during the first 2 weeks following SE, (2) significantly lower spontaneous seizure frequencies overall during the first month following SE, and (3) a shift in the proportion of convulsive seizures relative to non-convulsive seizures.

WP1066 reduces transcription of STAT3-target genes in dentate gyrus following SE

Enhanced activation of the transcription factor STAT3 in the DG could contribute to epileptogenesis by regulating genes involved in cellular proliferation, survival, differentiation, angiogenesis, and/or neurotransmitter receptor expression. An important goal of these studies was to identify the targets of STAT3-driven transcription that are elevated following status epilepticus in DG and determine whether WP1066 treatment prevents SE-induced transcription of these genes during early epileptogenesis (i.e., 6 h or 24 h after SE). Following SE, significant increases in c-myc mRNA levels (8.3-fold increase), mcl-1 mRNA levels (2.5-fold increase), and ICER mRNA (29.8-fold increase) were observed at 6 h relative to control rats (Fig 6A). In addition, several STAT3-target genes demonstrated increases 24 h after pilocarpine-induced SE (Fig 6B). C-myc and cyclin D1 (increasing 17.1-fold and 5.6-fold, respectively) are genes involved in cellular proliferation and differentiation (Dang, 1999; Bernard and Eilers, 2006; Stacey, 2003; Fu, 2004). Bcl-xl and mcl-1, two prosurvival genes (Lindsten et al., 2005; Kim, 2005; Yang-Yen, 2006), increased by 1.6-fold and 2.7-fold compared to control rats 24 h after SE. ICER, a member of the CREB family that has been shown to down-regulate the GABA(A) receptor α1 gene (*Gabra1*) after SE (Hu et al., 2008), increased by 16.6-fold 24 h after SE. The other STAT3

target genes investigated, bcl-2 and VEGF, did not demonstrate significant increases following SE at either timepoint (Fig. 6)

Studies analyzing the effect of STAT3 inhibition on downstream targets were conducted 24 h after SE when the most consistent increase in all genes induced by SE was observed. Interestingly, early and transient treatment with WP1066 significantly reduces SE-induced increases in cyclin D1 (by 58.3%) and mcl-1 (by 27.8%, [Fig 7]) suggesting that a potential effect on (1) cell cycle progression via cyclin D1 reduction and/or (2) prosurvival machinery via mcl-1 reduction in the DG may contribute to the disease modifying effects of WP1066. WP1066 did not significantly reduce ICER mRNA levels 24 h after SE. Potential WP1066 effects on SE-induced down-regulation of GABA (A) α1 subunit protein, a downstream target of ICER, were evaluated 24 h later (i.e., 48 h after SE). WP1066 administration did not significantly change GABA (A) α1 subunit protein levels 48 h after SE relative to vehicle-treated rats (SE+DMSO [n=3], 76.01% control immunoreactivity vs. SE+WP1066 [n=3], 73.87% control immunoreactivity; p=0.5655). WP1066 did not significantly reduce c-myc mRNA increases in the DG. Notably, c-myc is transcriptionally regulated by several other SE-activated signaling pathways other than JAK/STAT (e.g., mTOR and β-catenin [Crino, 2005; Orlova et al., 2010]), and induction of its transcription following SE by these pathways likely overwhelm any effects of the transient, partial reduction in pSTAT3 produced WP1066 administration.

WP1066 does not exacerbate SE-induced neuronal cell death in the hippocampus

WP1066 activates Bcl-2–associated X protein (i.e., Bax), which promotes apoptosis by competing with Bcl-2 proper, and WP1066 down-regulates several anti-apoptotic proteins selectively in human malignant glioma U87-MG and U373-MG cells treated for 72 h, but not in normal human astrocyte (NHA) cell lines (Iwamaru et al., 2007). In addition, some of the STAT3-target genes studied have been implicated in apoptosis. Thus, histological experiments were conducted to determine whether WP1066 treatment exacerbated cell death in the hippocampus of epileptic animals relative to vehicle-treated rats. Studies evaluating neuronal death 48 h after SE in the dentate hilus, CA1, and CA3 layers of the hippocampus demonstrate no difference in FlouroJade-B positive cell densities in rats treated with WP1066 compared to vehicle-treated rats (Fig 8). No FlouroJade B staining was observed in control rats that had not been subjected to SE. Additional studies evaluating potential differences in neuronal cell density >30 days after SE in the dentate hilus, CA1, and CA3 using NeuN, an antibody specific for neuronal nuclear protein were also performed. No significant difference was detected in the mean neuronal cell density (based on NeuN immunopositive neuronal cell counts) in dentate hilus or CA3 of animals subjected to SE and treated with WP1066 (50 mg/kg at onset of SE and a second 50 mg/kg dose 45 minutes later (n=4, dentate hilus=139.8 ± 16.2 NeuN positive neurons/mm^2, CA3=218.5 ± 56.4 NeuN positive neurons/mm^2), relative to animals treated with DMSO at onset of SE and sacrificed >30 days later (n=4, dentate hilus=156.1 ± 18.4 NeuN positive neurons/mm^2, CA3=240.3 ± 35.8 NeuN positive neurons/mm^2). Both treatment groups demonstrated significantly lower neuronal cell density in the dentate hilus (SE+DMSO=$p<0.01$; SE +WP1066=$p<0.001$) and CA3 (SE+DMSO=$p<0.05$; SE+WP1066=$p<0.01$) relative to controls (n=4; dentate hilus=214.7 ± 9.3 NeuN positive neurons/mm^2, CA3=332.8 ± 23.9 NeuN positive neurons/mm^2) >30 days after SE, but no significant difference in mean neuronal cell density was observed between any of the groups in CA1 at this time point (CTRL=129.5 ± 8.0 NeuN positive neurons/mm^2; SE+DMSO=113.1 ± 22.7 NeuN positive neurons/mm^2; SE + WP1066 = 141.1 ± 44.3 NeuN positive neurons/mm^2).

Discussion

WP1066 administration (100 mg/kg total i.p. in DMSO) at the onset of SE transiently inhibits the levels of pSTAT3 (without reducing SE) and reduces the severity of subsequent epilepsy (as evidence by suppressed spontaneous seizure frequency for up to 1 month) in an animal model of temporal lobe epilepsy. These data suggest that JAK/STAT inhibitors, once optimized, could be important disease-modifying agents with the potential to inhibit epilepsy development after brain insults such as prolonged seizures and possibly other forms of brain injury that are associated with JAK/STAT activation and can lead to epilepsy, such as trauma and stroke.

Caveats related to WP1066 pharmacokinetics

WP1066 was originally developed for cancer therapeutics and has not been optimized for use in neurological disorders. Although it does have some blood brain barrier (BBB) permeability, the very high dose required to obtain a CNS effect after peripheral administration *in vivo* vs. effective concentration *in vitro* suggests that either BBB permeability, metabolism, absorption or some combination thereof requires optimization for a compound like this to be of use for clinical indications. Two 50 mg/kg doses of WP1066 delivered at SE onset and 45 minutes later were required to overcome the compound's rapid clearance and inhibit early STAT3 phosphorylation in brain. Despite only transient levels of WP1066 *in vivo* in the brain and plasma, resulting in brief reduction of STAT3 phosphorylation, there was a dramatic reduction in the severity of later epilepsy. WP1066 treatment did not, however, completely prevent the development of epilepsy. The incomplete efficacy may be due, in part, to these fundamental pharmacokinetic problems with WP1066. Our data suggest that JAK/STAT inhibition can be disease modifying in epilepsy, and that development of novel compounds that overcome the unfavorable pharmacokinetic properties of WP1066 could lead to a new therapeutic approach to reduce or prevent epilepsy following brain injury.

Up-regulation of STAT3 target genes following SE and other brain insults

The JAK/STAT pathway has been extensively studied in other disease processes, specifically cancer and inflammatory disorders, and a number of the genes that have been identified as STAT3 targets in those studies are also implicated in pathological processes that may be important to epileptogenesis. The proliferation of tumor cells is mediated via STAT3 inducing the expression of cyclin D1 (Masuda et al., 2002). STAT3 upregulates the expression of several genes associated with growth and/or proliferation such as c-myc (Kiuchi et al., 1999), and antiapoptotic, prosurvival genes such as bcl-2 (Zushi et al., 1998), bcl-xl (Catlett-Falcone et al., 1999; Bromberg et al., 1999), and mcl-1 (Liu et al., 2003). STAT3 activation increases the proangiogenic factor vascular endothelial growth factor (VEGF [Niu et al., 2002]). Activation of the JAK/STAT pathway after SE causes increased transcription of ICER and subsequent down-regulation of the $GABA_A$ receptor α1 subunit 24 h later (Lund et al., 2008). Thus, we aimed to investigate whether STAT3-driven gene transcription, well documented in tumor cells, is also active following SE and whether early inhibition of STAT3 phosphorylation could suppress increased expression of mRNA levels of STAT3 target genes in the DG during early epileptogenesis (i.e., 6 h or 24 h after SE).

In our study, we found that levels of c-myc, mcl-1, and ICER mRNA were significantly increased at 6 h and 24 h after SE, and that cyclin D1 and bcl-xl were increased 24 h after SE. Elevated mcl-1 mRNA levels have previously been observed in the dentate gyrus 12 h after pilocarpine-induced SE in C57BL/6 mice (Mori et al., 2004). Previous reports on the expression of bcl-2 family of anti-apoptotic proteins in epilepsy are conflicting. Similar to our results, significantly higher protein levels of antiapoptotic bcl-2 and bcl-xl have been

observed in the neocortex of TLE patients with intractable seizures compared to autopsy controls and levels of bcl-xl correlate with patient seizure frequency (Henshall et al., 2000). However, following kainate-induced SE in mice, the prosurvival protein bcl-2 is down-regulated and it's partner, proapoptotic bax protein is up-regulated (Gillardon et al., 1995). Bcl-2 and bcl-xl were equally expressed in dying and surviving neurons following kainate-induced SE, but bax protein and mRNA expression increased progressively over time in susceptible neurons (Lopez et al., 1999). Unlike the robust increases in c-myc reported here, previous literature suggests no change or a down-regulation of c-myc following repeated electroconvulsive seizures, kainate-induced SE, and kindled seizures (Jeon, WJ et al., 2008; Azuma, Y. et al., 1996; Simonato M. et al., 1991). Cyclin D1 mRNA increases have been reported following transient global ischemia and kainate-induced seizures in neurons vulnerable to cell death in the CA1, CA3, and DG cell layers of the hippocampus (Timsit, 1999) and in the hippocampus of the El mouse, an epileptic mutant, prior to the onset of spontaneous seizures (Murashima, 2007). Others report increased cyclin D1 expression in CA1 pyramidal cells may increase susceptibility to PTZ and kainate-induced seizures and excitotoxic cell death, but show cyclin D1 is not a direct participant in apoptosis. (Koeller et al., 2008). VEGF protein has been reported to increase in both neurons and glia following pilocarpine-induced SE (Croll et al., 2004). Potential conflicts in results reported in the different studies analyzing expression of downstream targets of STAT3 are likely dependent on the animal model used, the time points studied, and brain region analyzed. Characterization of the timecourse of region- and cell-specific mRNA and protein expression following pilocarpine-induced SE is required to better understand the role these STAT3 targets may play in epileptogenesis.

Potential disease-modifying mechanisms of WP1066

Using the current administration protocol, systemic administration of WP1066 transiently reduces seizure-induced pSTAT3 *in vivo* and has a disease modifying effect, with WP1066-treated rats having lower daily seizure frequencies over time relative to vehicle-treated rats. Downstream signaling of pSTAT3 following WP1066 administration was evaluated to further delineate potential mechanisms of the WP1066 effects. The JAK/STAT pathway regulates the expression of genes involved in pro-survival, anti-apoptotic, and proliferative machinery, in both neurons and glia; thus, inhibition of this pathway may impact a number of mechanisms that are important for the development and progression of epilepsy including aberrant, seizure-induced neurogenesis, reactive gliosis, and mossy fiber sprouting. WP1066 prevents the SE-induced upregulation of cyclin D1 and mcl-1, downstream targets of STAT3, in the dentate gyrus 24 h after administration despite its poor stability and limited CNS penetration.

Cyclin D1 is a member of the the G1 cyclins and plays an important role in the cell cycle in proliferating cells via activation of cyclin-dependent kinases (e.g., CDK2, CDK4, or CDK6) which phosphorylate and inactivate the retinoblastoma protein and promotes progression through the G_1-S phase of the cell cycle (Fu et al., 2004). Activation of cyclin D1, and the corresponding CDK family, has been associated with an increased number of BrdU positive cells in EL mice during epileptogenesis (Y.L. Murashima et al., 2007). The activation of Cyclin D1 during early stages of pilocarpine-induced epileptogenesis could thus be promoting the enhanced cell proliferation known to occur in the dentate gyrus after SE (Ribak and Dashtipour 2002; Cha et al., 2004; Mohapel et al., 2004; Parent, 2003; Scharfman, 2004).

After TBI in rats (i.e., fluid percussion injury), administration of cell-cycle inhibitors that reduced cyclin D1 expression in neurons and glia in the hippocampus, decreased neuronal cell death and lesion volume, reduced reactive astrogliosis, microglial activation, and

improved motor and cognitive recovery (Di Giovanni et al., 2005). Likewise, cyclin D1 knockout mice exposed to controlled cortical impact demonstrate reduced cell cycle activation, and reduced neurodegeneration 24 h after injury and also showed improved cognitive function, reduced hippocampal neuronal cell loss, decreased lesion volume, and cortical microglial activation 21 days after controlled cortical impact (CCI) injury (Kabadi et al., 2012).

In addition to the role of cyclin D1 in cell proliferation, growth, and differentiation, it can also trigger apoptosis following ischemia and kainate-induced SE and it has been suggested that increased cyclin D1 is associated with programmed cell death (Pollard et al., 1994, Freeman, 1994). These contrasting findings imply that Cyclin D1 can induce different effects depending on cellular factors, such as cell type and intracellular or extracellular cues (e.g., presence or absence of growth factors). Partial inhibition of cyclin D1 with the STAT3 inhibitor, WP1066, does not appear to be neuroprotective based on counts of FlouroJade B positive neuronal cell densities in hippocampal cell layers.

Mcl-1 (myeloid cell leukemia-1) is a bcl-2-related anti-apoptotic protein and is a key regulator of apoptosis during CNS development and DNA damage. High levels of mcl-1 protect against DNA damage and neuronal degeneration after injury (Arbour et al., 2008) and regulate the survival of adult neural precursor cells (Malone et al., 2012) in the subventricular zone (SVZ). Elevated mcl-1 mRNA levels have been reported in multiple limbic areas including CA1 pyramidal cells and DG granule cells after pilocarpine-induced SE in C57BL/6 mice (Mori et al., 2004). It is unknown what role mcl-1 may play in promoting neurogenesis in epilepsy or whether mcl-1 is present in glia after SE, possibly promoting the survival of reactive astroglia and progressive gliosis.

Current findings suggest potential candidate mechanisms by which STAT3 inhibition may impact epileptogenisis, but there are likely others. STAT 3 is known to be a crucial mediator of astroglial development and has recently been shown to increase oxidative phosphorylation and mitochondrial respiration (Gough et al., 2009: Reich, 2009). Thus, inhibition of STAT3 could be exerting its disease-modifying effects by impacting astrocyte activation and/or preventing mitochondrial dysfunction. Determining the exact mechanism or combination of mechanisms mediating the disease modifying effects of STAT3 inhibition will require additional investigation.

Inhibition of pSTAT3 as a potential therapeutic strategy

Results of these studies provide the first proof-of-principle that inhibiting STAT3 phosphorylation may be a novel therapeutic approach to inhibit primary epileptogenesis after brain injury and to reduce severity of acquired epilepsy. The administration paradigm used in these studies did not employ intrahippocampal delivery or a pretreatment, but instead, administered WP1066 i.p. following the onset of SE, a more therapeutically relevant time point for clinical practice, because it is impossible to predict when a brain insult will occur, making administration of the drug prophylactically impractical. A STAT3 inhibitor with greater stability and CNS penetration may demonstrate a greater disease modifying effect than that seen with WP1066 in our current studies. Development of stable compounds with optimized pharmacokinetics to inhibit STAT3 phosphorylation in brain may lead to true disease modifying therapies that do not just symptomatically treat seizures but inhibit their development and progression. It should be noted, however, that kinase inhibitors are notoriously nonspecific. Despite evidence of selective inhibition of some STAT3 gene targets (Fig 7), the effects on spontaneous seizure frequency observed in this study may also be due to off-target effects and potential inhibition of other pro-epileptogenic signal pathways. Compounds that block STAT3 have also been shown to target other signaling pathways mediated by, for example, NF-κβ, MAPK and AKT (Mankan, 2011), the

downstream affects of which are extensive in the context of epileptogenesis. More specifically, WP1066 reduces p-AKT and β-catenin expression in human glioblastoma cell lines (Wang, 2011). These off-target effects may limit the usefulness of STAT3 inhibitory compounds, or could be leveraged to accomplish a broad-spectrum inhibition of multiple activity-dependent, signal pathways that are activated by prolonged seizures as well as other brain insults that can lead to epilepsy, such as traumatic brain injury (Oliva et al, 2011; Zhao et al., 2011; Raible et al., 2011) and stroke (Planas et al., 1996; Suzuki et al, 2001). STAT3 inhibitors may, thus, have therapeutic value as adjunctive therapies to abort pathway activation immediately following a variety of brain insults or injuries to inhibit the development and progression of acquired epilepsy.

Acknowledgments

The authors would like to thank Dr. Yogendra Raol and the University of Colorado Neurophysiology Core for assistance related to EEG monitoring and Dana Hund for technical assistance with histology. These studies were funded by NIH, National Institute of Neurological Disorders and Stroke R01NS051710 (to ABK and SJR), Citizens United for Research in Epilepsy [(CURE) to ABK and SJR], Epilepsy Foundation (to HG), NIH/NCATS Colorado Clinical Translational Science Award UL1 RR025780 (to the University of Colorado Medicinal Chemistry Core), and the Colorado Center for Drug Discovery (to ABK and MFW).

Abbreviations

JAK	Janus Kinase
STAT	Signal Transducer and Activator of Transcription
ICER	Inducible cAMP Early Repressor protein
c-myc	cellular regulatory gene that codes for a transcription factor
mcl-1	Induced myeloid leukemia cell differentiation protein
bcl-2	B-cell lymphoma 2
bcl-xl	B-cell lymphoma-extra large
Cyclin D1	G1/S-specific cyclin-D1 (encoded by *CCND1*)
VEGF	Vascular endothelial growth factor

References

Aaronson DS, Horvath CM. A road map for those who don’t know JAK-STAT. Science. 2002; 296:1653–5. [PubMed: 12040185]

Arbour N, et al. Mcl-1 is a key regulator of apoptosis during CNS development and after DNA damage. J Neurosci. 2008; 28:6068–78. [PubMed: 18550749]

Azuma Y, et al. Particular nuclear transcription factors responsive to systemic administration of kainic acid in murine brain. Neurochem Int. 1996; 29:289–99. [PubMed: 8885288]

Balish M, et al. Seizure frequency in intractable partial epilepsy: a statistical analysis. Epilepsia. 1991; 32:642–9. [PubMed: 1915170]

Bauer J, Burr W. Course of chronic focal epilepsy resistant to anticonvulsant treatment. Seizure. 2001; 10:239–46. [PubMed: 11466018]

Berg AT, et al. How long does it take for partial epilepsy to become intractable? Neurology. 2003; 60:186–90. [PubMed: 12552028]

Bernard S, Eilers M. Control of cell proliferation and growth by Myc proteins. Results Probl Cell Differ. 2006; 42:329–42. [PubMed: 16903216]

Blume WT. The progression of epilepsy. Epilepsia. 2006; 47(Suppl 1):71–8. [PubMed: 17044831]

Bromberg JF, et al. Stat3 as an oncogene. Cell. 1999; 98:295–303. [PubMed: 10458605]

Catlett-Falcone R, et al. Constitutive activation of Stat3 signaling confers resistance to apoptosis in human U266 myeloma cells. Immunity. 1999; 10:105–15. [PubMed: 10023775]

Cha BH, et al. Spontaneous recurrent seizure following status epilepticus enhances dentate gyrus neurogenesis. Brain Dev. 2004; 26:394–7. [PubMed: 15275703]

Choi JS, et al. Upregulation of gp130 and differential activation of STAT and p42/44 MAPK in the rat hippocampus following kainic acid-induced seizures. Brain Res Mol Brain Res. 2003; 119:10–8. [PubMed: 14597225]

Crino PB. Molecular pathogenesis of focal cortical dysplasia and hemimegalencephaly. J Child Neurol. 2005; 20:330–6. [PubMed: 15921235]

Croll SD, et al. Vascular endothelial growth factor (VEGF) in seizures: a double-edged sword. Adv Exp Med Biol. 2004; 548:57–68. [PubMed: 15250585]

Dang CV, et al. Function of the c-Myc oncogenic transcription factor. Exp Cell Res. 1999; 253:63–77. [PubMed: 10579912]

Darnell JE Jr, et al. Jak-STAT pathways and transcriptional activation in response to IFNs and other extracellular signaling proteins. Science. 1994; 264:1415–21. [PubMed: 8197455]

Di Giovanni S, et al. Cell cycle inhibition provides neuroprotection and reduces glial proliferation and scar formation after traumatic brain injury. Proc Natl Acad Sci U S A. 2005; 102:8333–8. [PubMed: 15923260]

England MJ, et al. Epilepsy across the spectrum: promoting health and understanding. A summary of the Institute of Medicine report. Epilepsy Behav. 2012; 25:266–76. [PubMed: 23041175]

Ferrajoli A, et al. WP1066 disrupts Janus kinase-2 and induces caspase-dependent apoptosis in acute myelogenous leukemia cells. Cancer Res. 2007; 67:11291–9. [PubMed: 18056455]

Freeman RS, et al. Analysis of cell cycle-related gene expression in postmitotic neurons: selective induction of Cyclin D1 during programmed cell death. Neuron. 1994; 12:343–55. [PubMed: 8110463]

Fu M, et al. Minireview: Cyclin D1: normal and abnormal functions. Endocrinology. 2004; 145:5439–47. [PubMed: 15331580]

Gillardon F, et al. Up-regulation of bax and down-regulation of bcl-2 is associated with kainate-induced apoptosis in mouse brain. Neurosci Lett. 1995; 192:85–8. [PubMed: 7675327]

Gough DJ, et al. Mitochondrial STAT3 supports Ras-dependent oncogenic transformation. Science. 2009; 324:1713–6. [PubMed: 19556508]

Haut SR, et al. Chronic disorders with episodic manifestations: focus on epilepsy and migraine. Lancet Neurol. 2006; 5:148–57. [PubMed: 16426991]

Haut SR, et al. Seizure clustering during epilepsy monitoring. Epilepsia. 2002; 43:711–5. [PubMed: 12102673]

Henshall DC, et al. Alterations in bcl-2 and caspase gene family protein expression in human temporal lobe epilepsy. Neurology. 2000; 55:250–7. [PubMed: 10908900]

Hu Y, et al. Surface expression of GABAA receptors is transcriptionally controlled by the interplay of cAMP-response element-binding protein and its binding partner inducible cAMP early repressor. J Biol Chem. 2008; 283:9328–40. [PubMed: 18180303]

Hussain SF, et al. A novel small molecule inhibitor of signal transducers and activators of transcription 3 reverses immune tolerance in malignant glioma patients. Cancer Res. 2007; 67:9630–6. [PubMed: 17942891]

Ihle JN. STATs: signal transducers and activators of transcription. Cell. 1996; 84:331–4. [PubMed: 8608586]

Iwamaru A, et al. A novel inhibitor of the STAT3 pathway induces apoptosis in malignant glioma cells both in vitro and in vivo. Oncogene. 2007; 26:2435–44. [PubMed: 17043651]

Jeon WJ, et al. Repeated electroconvulsive seizure induces c-Myc down-regulation and Bad inactivation in the rat frontal cortex. Exp Mol Med. 2008; 40:435–44. [PubMed: 18779656]

Kabadi SV, et al. Cyclin D1 gene ablation confers neuroprotection in traumatic brain injury. J Neurotrauma. 2012; 29:813–27. [PubMed: 21895533]

Kim R. Unknotting the roles of Bcl-2 and Bcl-xL in cell death. Biochem Biophys Res Commun. 2005; 333:336–43. [PubMed: 15922292]

Kiuchi N, et al. STAT3 is required for the gp130-mediated full activation of the c-myc gene. J Exp Med. 1999; 189:63–73. [PubMed: 9874564]

Koeller HB, et al. Cyclin D1 in excitatory neurons of the adult brain enhances kainate-induced neurotoxicity. Neurobiol Dis. 2008; 31:230–41. [PubMed: 18585919]

Kupferman ME, et al. Therapeutic suppression of constitutive and inducible JAK\STAT activation in head and neck squamous cell carcinoma. J Exp Ther Oncol. 2009; 8:117–27. [PubMed: 20192118]

Levy DE, Darnell JE Jr. Stats: transcriptional control and biological impact. Nat Rev Mol Cell Biol. 2002; 3:651–62. [PubMed: 12209125]

Lindsten T, et al. Defining the role of the Bcl-2 family of proteins in the nervous system. Neuroscientist. 2005; 11:10–5. [PubMed: 15632274]

Liu H, et al. Serine phosphorylation of STAT3 is essential for Mcl-1 expression and macrophage survival. Blood. 2003; 102:344–52. [PubMed: 12637318]

Lopez E, et al. Bcl-2, Bax and Bcl-x expression following kainic acid administration at convulsant doses in the rat. Neuroscience. 1999; 91:1461–70. [PubMed: 10391451]

Lund IV, et al. BDNF selectively regulates GABAA receptor transcription by activation of the JAK/STAT pathway. Sci Signal. 2008; 1:ra9. [PubMed: 18922788]

Malone CD, et al. Mcl-1 regulates the survival of adult neural precursor cells. Mol Cell Neurosci. 2012; 49:439–47. [PubMed: 22357134]

Mankan AK, Greten FR. Inhibiting signal transducer and activator of transcription 3: rationality and rationale design of inhibitors. Expert Opin Investig Drugs. 2011; 20:1263–75.

Masuda M, et al. Constitutive activation of signal transducers and activators of transcription 3 correlates with cyclin D1 overexpression and may provide a novel prognostic marker in head and neck squamous cell carcinoma. Cancer Res. 2002; 62:3351–5. [PubMed: 12067972]

Mohapel P, et al. Status epilepticus severity influences the long-term outcome of neurogenesis in the adult dentate gyrus. Neurobiol Dis. 2004; 15:196–205. [PubMed: 15006689]

Mori M, et al. Expression of apoptosis inhibitor protein Mcl1 linked to neuroprotection in CNS neurons. Cell Death Differ. 2004; 11:1223–33. [PubMed: 15286683]

Murashima YL, et al. Cell cycle reentry and cell proliferation as candidates for the seizure predispositions in the hippocampus of EL mouse brain. Epilepsia. 2007; 48(Suppl 5):119–25. [PubMed: 17910591]

Niu G, et al. Constitutive Stat3 activity up-regulates VEGF expression and tumor angiogenesis. Oncogene. 2002; 21:2000–8. [PubMed: 11960372]

Oliva AA Jr, et al. STAT3 signaling after traumatic brain injury. J Neurochem. 2011; 120:710–20. [PubMed: 22145815]

Orlova KA, et al. Early progenitor cell marker expression distinguishes type II from type I focal cortical dysplasias. J Neuropathol Exp Neurol. 2010; 69:850–63. [PubMed: 20613634]

Parent JM. Injury-induced neurogenesis in the adult mammalian brain. Neuroscientist. 2003; 9:261–72. [PubMed: 12934709]

Planas AM, et al. Induction of Stat3, a signal transducer and transcription factor, in reactive microglia following transient focal cerebral ischaemia. Eur J Neurosci. 1996; 8:2612–8. [PubMed: 8996811]

Pollard H, et al. Kainate-induced apoptotic cell death in hippocampal neurons. Neuroscience. 1994; 63:7–18. [PubMed: 7898662]

Racine RJ. Modification of seizure activity by electrical stimulation. II. Motor seizure. Electroencephalogr Clin Neurophysiol. 1972; 32:281–94. [PubMed: 4110397]

Raible DJ, et al. GABA(A) Receptor Regulation after Experimental Traumatic Brain Injury. J Neurotrauma. 2011

Reich NC. STAT3 revs up the powerhouse. Sci Signal. 2009; 2:pe61. [PubMed: 19797267]

Ribak CE, Dashtipour K. Neuroplasticity in the damaged dentate gyrus of the epileptic brain. Prog Brain Res. 2002; 136:319–28. [PubMed: 12143392]

Scharfman HE. Functional implications of seizure-induced neurogenesis. Adv Exp Med Biol. 2004; 548:192–212. [PubMed: 15250595]

Schindler C, Darnell JE Jr. Transcriptional responses to polypeptide ligands: the JAK-STAT pathway. Annu Rev Biochem. 1995; 64:621–51. [PubMed: 7574495]

Shukla G, Prasad AN. Natural history of temporal lobe epilepsy: antecedents and progression. Epilepsy Res Treat. 2012; 2012:195073. [PubMed: 22937237]

Simonato M, et al. Differential expression of immediate early genes in the hippocampus in the kindling model of epilepsy. Brain Res Mol Brain Res. 1991; 11:115–24. [PubMed: 1661808]

Stacey DW. Cyclin D1 serves as a cell cycle regulatory switch in actively proliferating cells. Curr Opin Cell Biol. 2003; 15:158–63. [PubMed: 12648671]

Suzuki S, et al. Phosphorylation of signal transducer and activator of transcription-3 (Stat3) after focal cerebral ischemia in rats. Exp Neurol. 2001; 170:63–71. [PubMed: 11421584]

Timsit S, et al. Increased cyclin D1 in vulnerable neurons in the hippocampus after ischaemia and epilepsy: a modulator of in vivo programmed cell death? Eur J Neurosci. 1999; 11:263–78. [PubMed: 9987030]

Wang Y, et al. Inhibition of STAT3 reverses alkylator resistance through modulation of the AKT and beta-catenin signaling pathways. Oncol Rep. 2011; 26:1173–80. [PubMed: 21887474]

Xu Z, et al. Role of signal transducer and activator of transcription-3 in up-regulation of GFAP after epilepsy. Neurochem Res. 2011; 36:2208–15. [PubMed: 21833841]

Yang-Yen HF. Mcl-1: a highly regulated cell death and survival controller. J Biomed Sci. 2006; 13:201–4. [PubMed: 16456709]

Zhao JB, et al. Activation of JAK2/STAT pathway in cerebral cortex after experimental traumatic brain injury of rats. Neurosci Lett. 2011; 498:147–52. [PubMed: 21596098]

Zhong Z, et al. Stat3 and Stat4: members of the family of signal transducers and activators of transcription. Proc Natl Acad Sci U S A. 1994; 91:4806–10. [PubMed: 7545930]

Zhong Z, et al. Stat3: a STAT family member activated by tyrosine phosphorylation in response to epidermal growth factor and interleukin-6. Science. 1994; 264:95–8. [PubMed: 8140422]

Zushi S, et al. STAT3 mediates the survival signal in oncogenic ras-transfected intestinal epithelial cells. Int J Cancer. 1998; 78:326–30. [PubMed: 9766567]

Highlights

1. WP1066 administration at the onset of status epilepticus (SE) transiently inhibits the levels of pSTAT3.
2. Early treatment with WP1066 does not alter electrographic status epilepticus.
3. WP1066 reduces the severity and frequency of spontaneous seizures for up to 1 month after pilocarpine-induced SE.
4. WP1066 reduces transcription of STAT3-target genes in dentate gyrus following SE, specifically mcl-1 and cyclin D1.
5. WP1066 does not reduce or exacerbate seizure-induced neuronal cell death in the hippocampus acutely or chronically after SE.

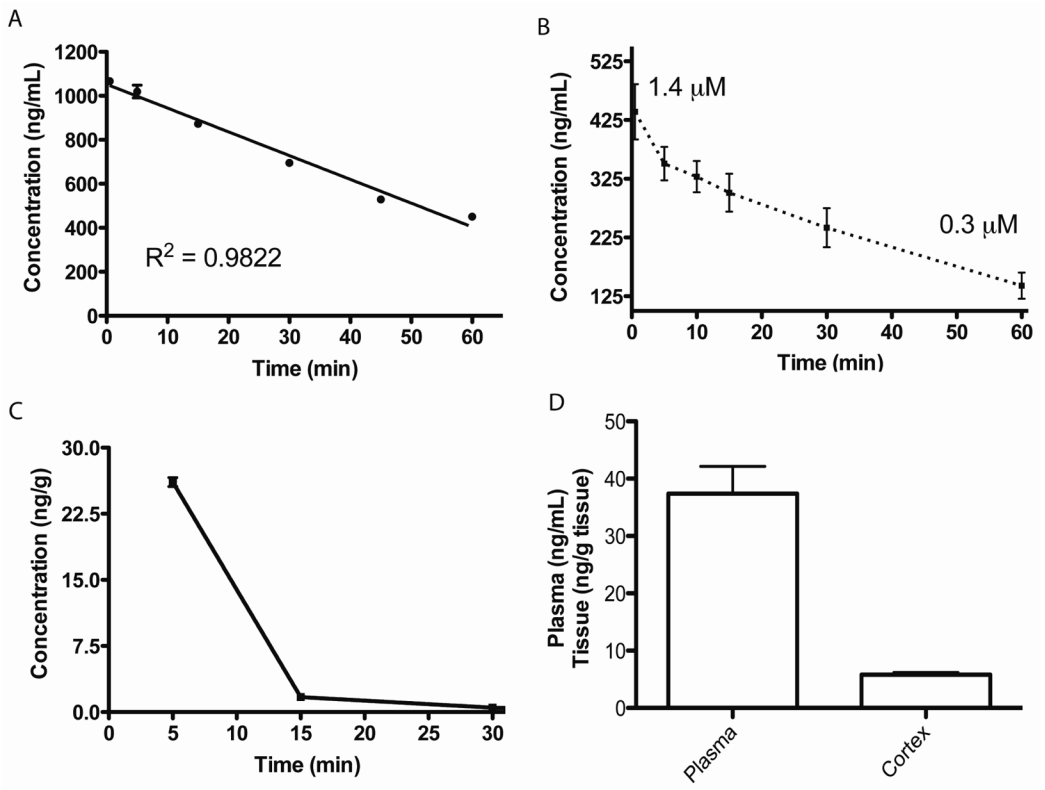

Fig. 1. WP1066 exhibited fast kinetics *in vivo* and *in vitro*

(A) WP1066 (100 mg/kg) has an apparent *in vitro* rat (Sprague-Dawley) plasma half-life (37 °C) of ~1.0 hr (n=1 per time point). **(B)** *In vitro* incubation of WP1066 (100 mg/kg) with rat liver microsomes (0.2 mg/mL) and NADPH (2.0 mM) illustrates that WP1066 has moderate stability (n= 3). **(C)** WP1066 (100 mg/kg) administered i.p. to a normal rat is present in the brain at low concentrations 5 minutes post-dose *in vivo* and clearance is very fast. **(D)** Cortex and plasma harvested from animals receiving 50 mg/kg WP1066 at onset of SE, a second 50 mg/kg WP1066 dose 45 minutes later, and sacrificed 1 h after SE onset (15 minutes after second WP1066 dose, n=8) demonstrate some blood-brain permeability but relatively low brain and plasma concentrations. Error bars, mean±SD.

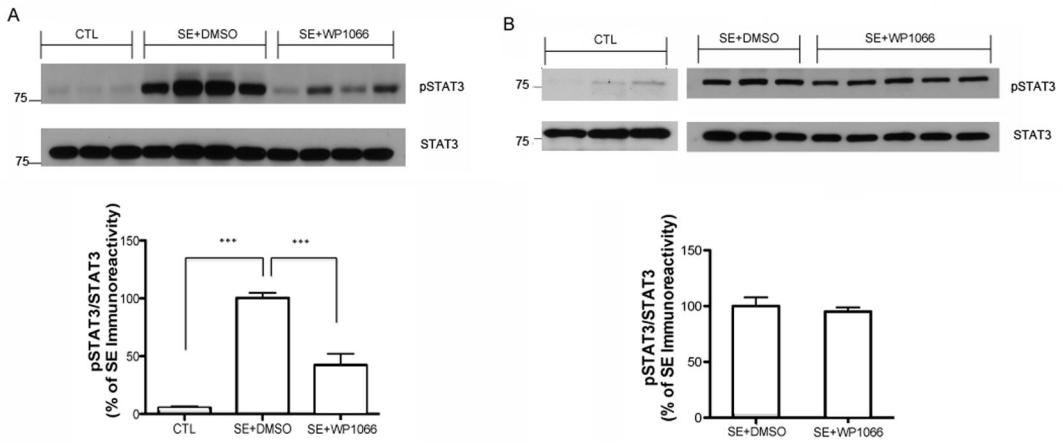

Fig. 2. WP1066 transiently inhibits SE-induced increases in STAT3 phosphorylation

Western blot of protein homogenates from DG of rats **(A)** 1 h and **(B)** 6 h after onset of SE probed with anti-pSTAT3 and STAT3 antibodies. 50 mg/kg of WP1066 (SE+WP1066) or vehicle (SE+DMSO) was injected i.p. at the onset of SE and again 45 minutes later. Control animals (CTL) received a sub-convulsive pilocarpine dose and did not experience SE. The ratio of pSTAT3/STAT3 was expressed as % change relative to mean values of the SE +DMSO group at each time point. WP1066 reduced SE-induced phosphorylation of STAT3 by ~58% 1 h after onset of SE (SE+DMSO, n=4; SE+WP1066, n=4), but no difference was demonstrated in the DG of WP1066-treated rats relative to DMSO-treated rats 6 h after the onset of SE (SE+DMSO, n=3; SE+WP1066, n=5).

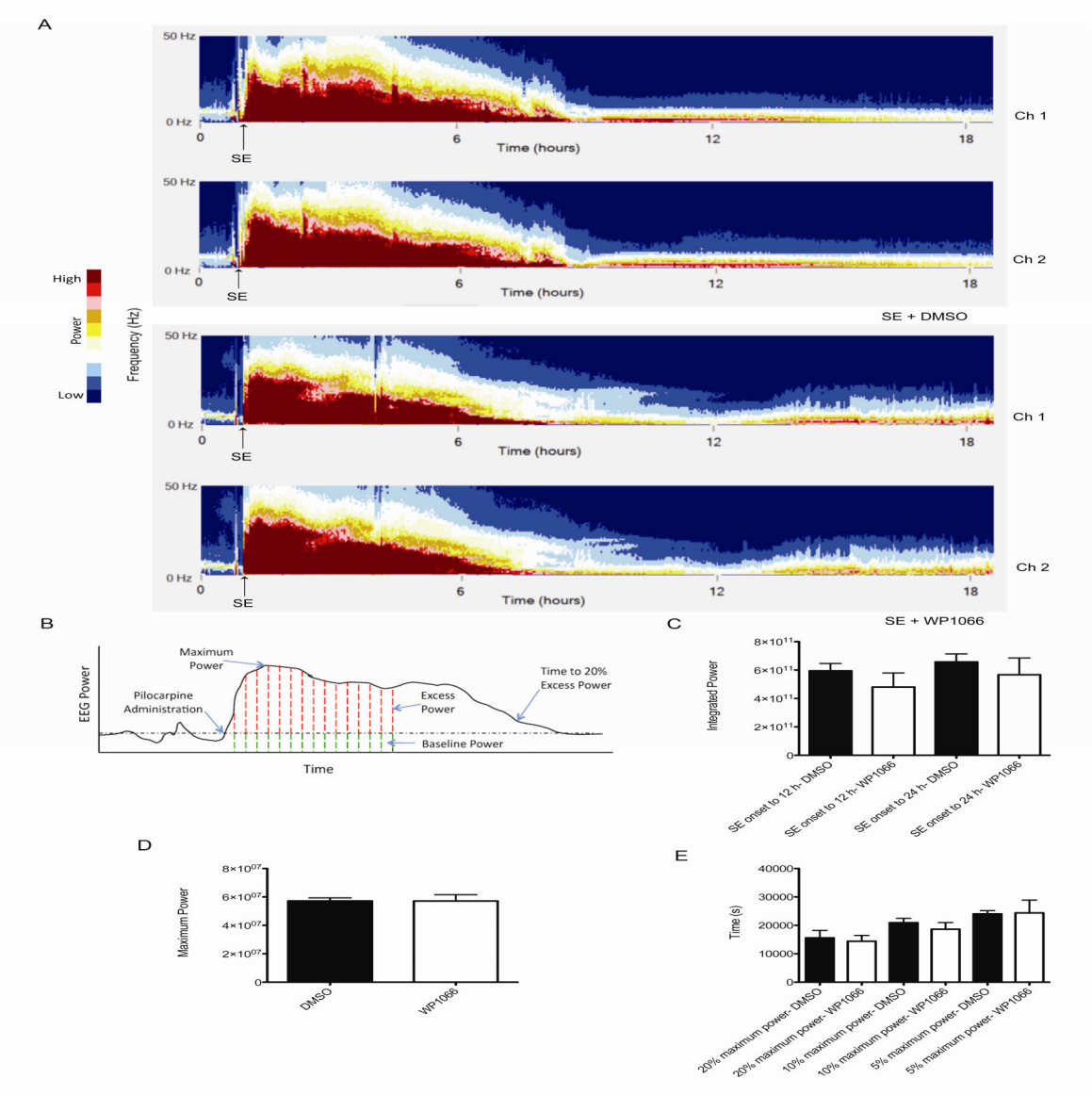

Fig. 3. WP1066 does not alter electrographic status epilepticus

Rats were continuously video-EEG monitored during and after pilocarpine-induced SE to conduct quantitative analyses of electrographic SE. 50 mg/kg of WP1066 (JAK/STAT Inhibitor) or vehicle (DMSO) was injected i.p. at the onset of SE and 50 mg/kg of the same treatment was administered again 45 minutes later. **(A)** Representative compressed spectral analyses (CSAs) are shown for the first ~19 hs following start of recording (including the time of pilocarpine administration. CSAs demonstrate magnitude power in low frequencies (0–50 Hz) over time following the onset of SE in animals implanted with 2 cortical EEG-recording electrodes treated with either vehicle (top 2 spectrographs) or WP1066 (bottom 2 spectrographs). Color map represents intensity of power graded from dark blue (lower magnitude) to dark red (higher magnitude). **(B)** Schematic describing indices of electrographic SE that were evaluated in these studies. Quantities determined include the maximum power, integrated power (the sum of red and green area), and the time to decrease from maximum power to 20% of the difference between maximum power and baseline power **(C)** Progression of SE shown by integrated power quantified at 12 h and 24 h after

the onset of SE. No significant differences were noted between DMSO-treated and WP1066-treated rats during the progression of SE. Maximum power **(D)** and the degradation of maximum power **(E)** were quantified to evaluate the intensity and duration of SE. No significant differences were detected between treatment and vehicle groups. (SE+DMSO, n=3, 6 channels; SE+WP1066, n=4, 8 channels). Error bars, ±SEM.

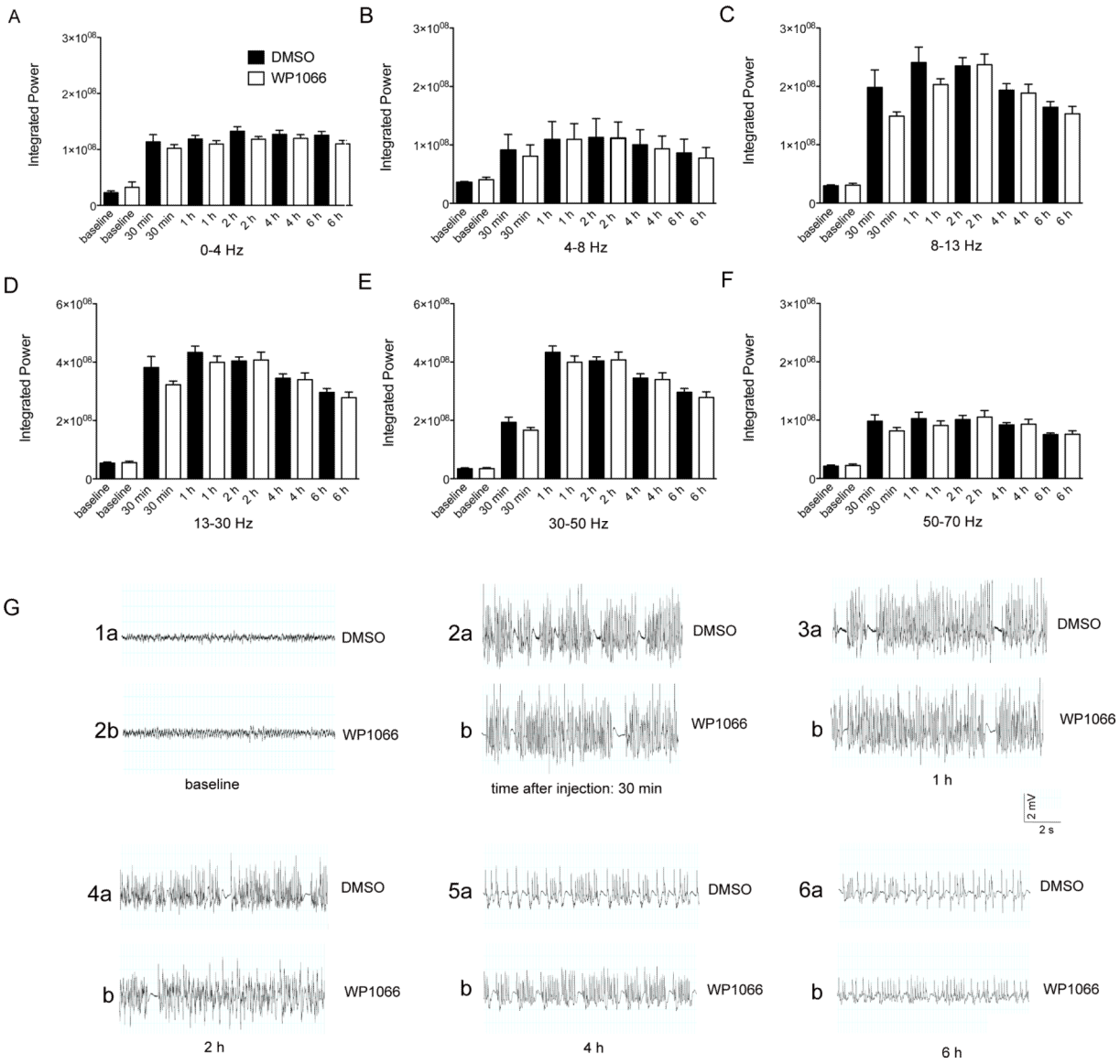

Fig 4. WP1066 does not have acute effects on discrete EEG bandwidths during SE

Integrated power was measured for baseline periods prior to induction of SE, and periods 30 min, 1 h, 2 h, 4 h, and 6 h after onset of SE and administration of WP1066 (50 mg/kg at onset of SE, and a second dose of 50 mg/kg 45 minutes later) or DMSO for **(A)** delta, **(B)** theta, **(C)** alpha, **(D)** 13–30 Hz, **(E)** 30–50 Hz, and **(F)** 50–70 Hz bandwidths. No significant difference was present at any time point following drug administration or within any EEG bandwidth between signals from WP1066-treated rats and DMSO-treated rats. Potential significant differences were evaluated using a using one-way ANOVA with Tukey's test for multiple comparisons. Representative traces sampled from a DMSO-treated rat **(G1a-6a)** and WP1066-treated rat **(G1b-6b)** at baseline (1 h prior to scopolamine administration), and at 30 min, 1 h, 2 h, 4 h, and 6 h following drug or vehicle injection demonstrate no alteration in the progression of pilocarpine-induced electrographic SE by treatment (SE+DMSO, n=3 rats; SE+WP1066, n=4 rats). Error bars, ±SEM.

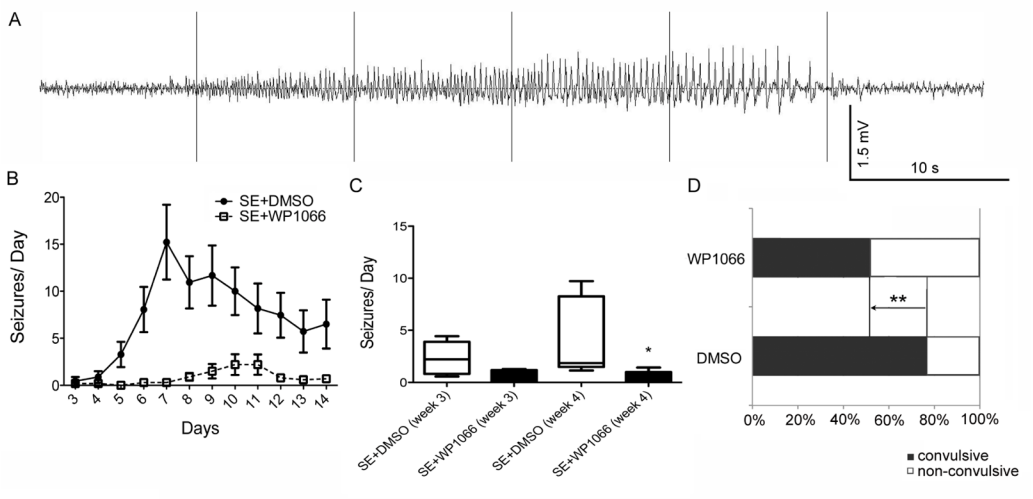

Fig 5. WP1066 alters the severity of pilocarpine-induced epilepsy

(A) A representative trace of a spontaneous electrographic seizure in a rat with pilocarpine-induced epilepsy. **(B)** The mean number of spontaneous seizures per day (at daily intervals) over the course of two weeks after SE demonstrates a progressive increase in spontaneous seizure frequency over time after SE in vehicle (DMSO)-treated rats (n=18) relative to rats treated with 50 mg/kg WP1066 at onset of SE and 50 mg/kg WP1066 45 min later (n=10). Statistical analysis was carried out using a two-way ANOVA accounting for time and treatment effects. WP1066 significantly effected the progression of seizure frequency over the first two weeks after SE (***$p<0.001$), and time also impacted the frequency of daily seizures ($p=0.0254$) over the first two weeks. **(C)** Three and four weeks after SE, WP1066-treated rats (n=6) still exhibit a lower daily seizure frequency relative to DMSO-treated rats (n=8). Statistically significant differences were determined using a one-way ANOVA with Tukey's test for multiple comparisons (*$p<0.05$). Box-and-whiskers plots. Upper and lower extremes of box are 75th and 25th percentiles. Whiskers extend from maximum value to minimum value. Line in box is plotted at median. (**D)** WP1066-treated rats demonstrate a significantly lower proportion of convulsive seizures (48.5 %) relative to DMSO-treated rats (76.6%). Statistically significant differences in the proportion of convulsive to non-convulsive seizures following WP1066 relative to vehicle treatment was determined using a Fischer's exact test (**$p<0.01$). Error bars, ±SEM for all graphs except (C).

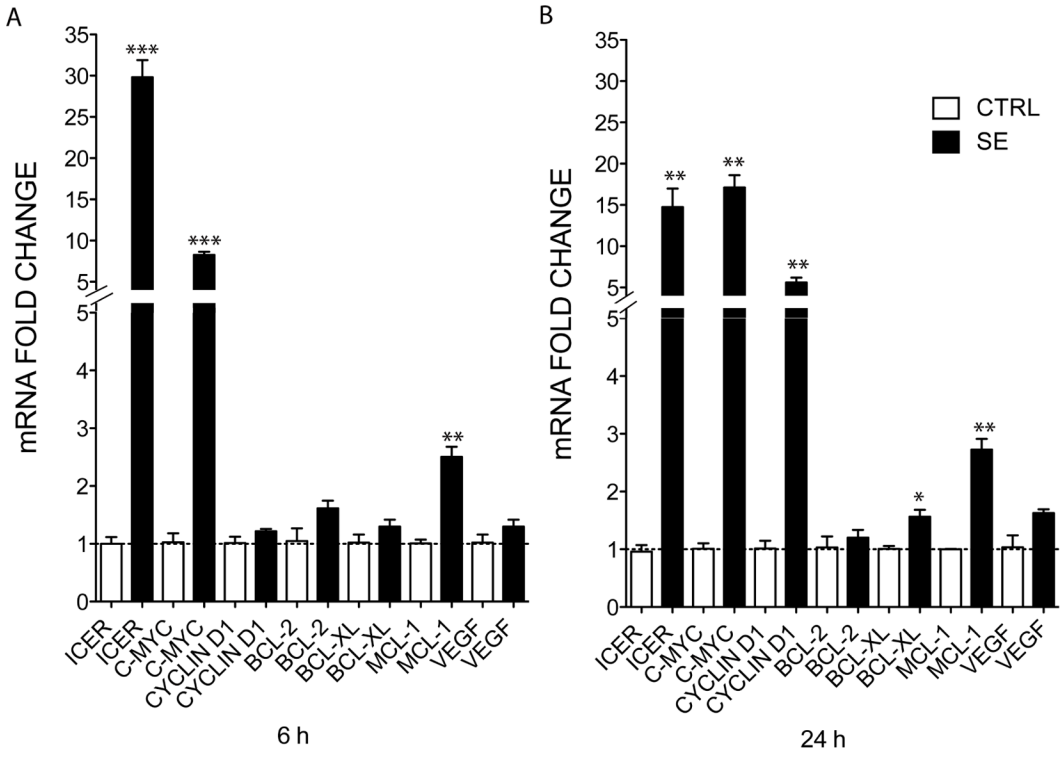

Fig 6. SE induces increases in STAT3-target genes

(A) Quantification of RT-PCR analysis of c-myc (CTRL, n=3; SE, n=4), cyclin D1 (CTRL, n=3; SE, n=4), bcl-2 (CTRL, n=3; SE, n=4), bcl-xl (CTRL, n=3; SE, n=4), mcl-1 (CTRL, n=3; SE, n=4), VEGF (CTRL, n=3; SE, n=4), and ICER (CTRL, n=5; SE, n=5) mRNA expression in DG 6 h after SE and **(B)** 24 h after SE (all genes, CTRL, n=3; SE, n=4). For RT-PCR reactions, each sample was run in triplicate**. (A)** SE caused a significant increase in ICER ($p<0.001$), c-myc ($p<0.001$), and mcl-1 ($p<0.01$) mRNA expression in DG of rats 6 h compared to CTRL. **(B)** SE induced significant increases in ICER ($p<0.01$), c-myc ($p<0.01$), cyclin D1 ($p<0.01$), bcl-xl ($p<0.05$), and mcl-1 ($p<0.01$) 24 h after SE. No significant difference in Bcl-2 or VEGF mRNA was observed at 6 h or 24 h after SE relative to levels in control rats, although a trend towards an increase was present. Expression of mRNA was normalized to cyclophilin and expressed as fold change compared to controls (CTRL, defined as 1). Significant differences were determined using an unpaired, Student's t-test.

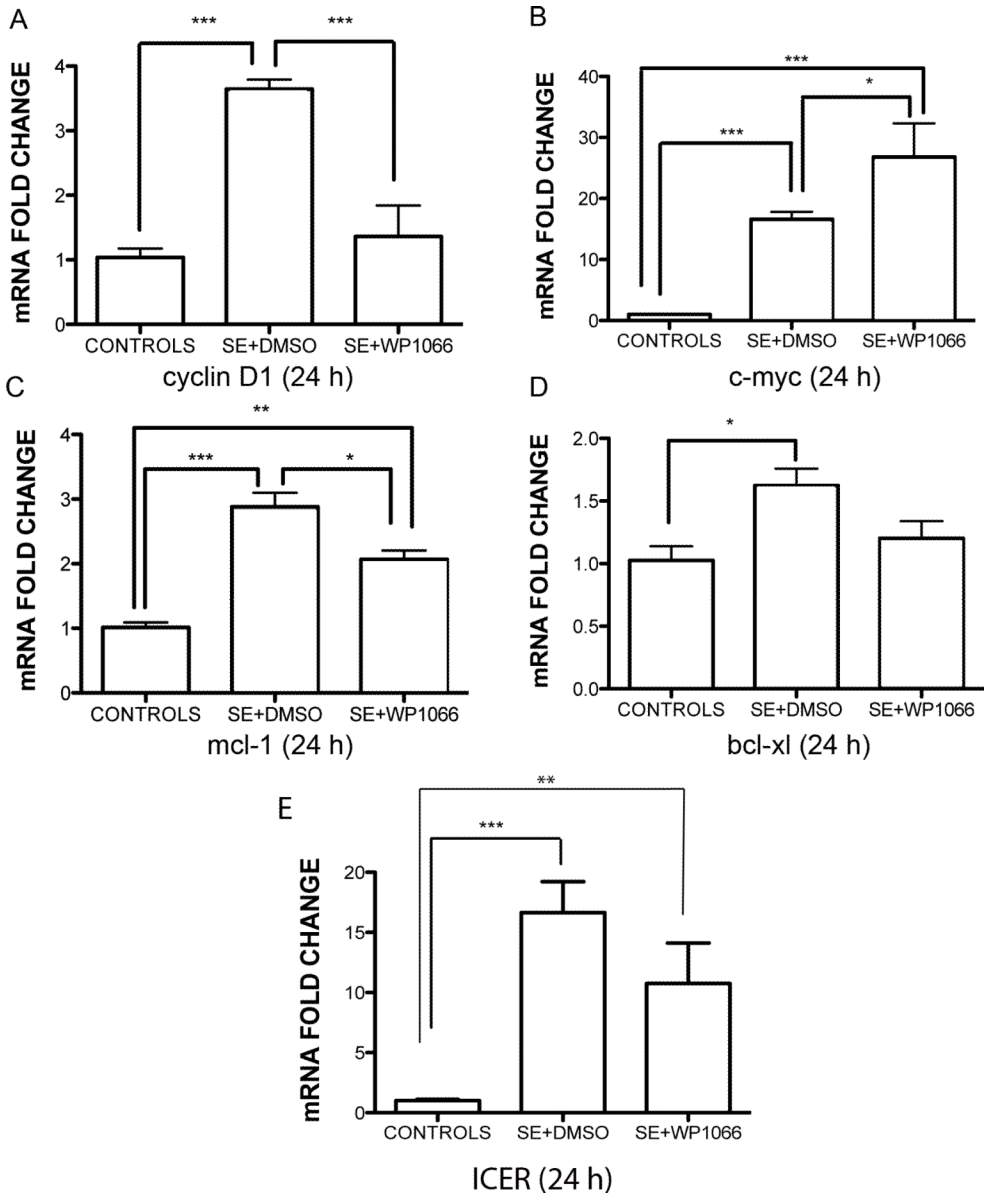

Fig 7. WP1066 inhibits SE-induced increases in STAT3-target genes

(A–E) RT-PCR quantification of cyclin D1, c-myc, mcl-1, bcl-xl, and ICER mRNA expression in dentate gyrus 24 h after SE and WP1066 or vehicle treatment (CTRL, n = 5; SE + DMSO, n = 6; SE + WP1066, n = 3 for all genes except ICER; and for ICER: CTRL, n=4; SE+DMSO, n=5; SE+WP1066, n=3). **(A)** Cyclin D1 mRNA expression was 58.3% lower ($p < 0.001$) inWP1066 treated rats 24 h after SE onset relative to vehicle treated rats. **(B)** WP1066 did not reverse increased expression of c-myc following status epilepticus in DG. **(C)** Mcl-1 mRNA expression was significantly reduced ($p < 0.05$) 24 h after SE in DG of WP1066-treated rats compared to vehicle-treated rats. **(D)** The administration of WP1066 at onset of SE did not significantly reduce the over-expression of bcl-xl or **(E)** ICER mRNA 24 h later in the DG. Expression of mRNA for all genes was normalized to cyclophilin and expressed as fold change compared to controls (CTL, defined as 1). Statistically significant differences in protein levels described above were determined using one-way ANOVAs with Tukey's tests for multiple comparisons. Error bars, mean ± S.E.M.

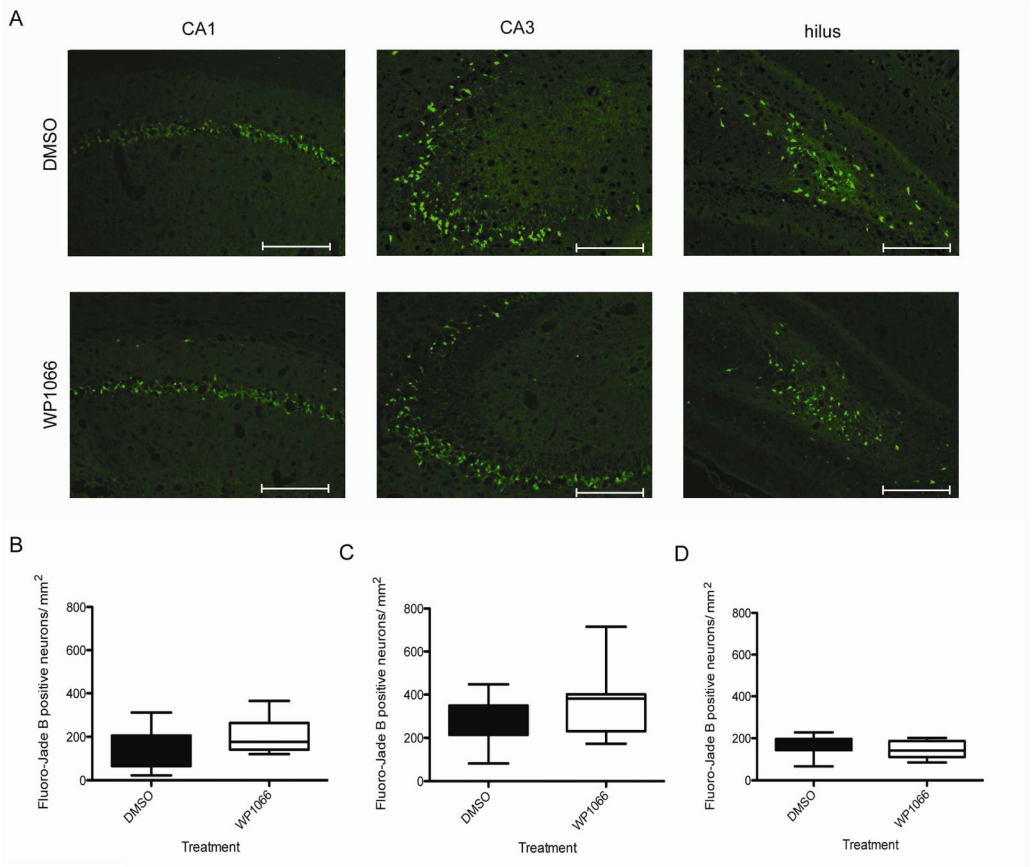

Fig 8. WP1066 does not reduce or exacerbate SE-induced neuronal cell death in hippocampus

(A) Representative images of Fluorojade-B stained CA1, CA3, and dentate hilus subregions from a DMSO-treated (n=11) or WP1066-treated rat (n=9) 48 hs after SE. Acquired using 10X objective on Nikon Eclipse TE2000-U fluorescent microscope. Calibration bars, 200 μm. Mean Fluorojade-B positive neuronal cell densities (i.e., positively stained neuronal cells per mm^2) averaged across a 1-in-20 series of serially sectioned and stained coronal sections (twenty 12-μm sections per rat) did not differ between WP1066-treated rats and DMSO-treated rats in (B) CA1, (C) CA3, or (D) dentate hilus. Potential statistically significant differences were determined using Mann-Whitney test. Box-and-whiskers plots, upper and lower extremes of box are 75^{th} and 25^{th} percentiles. Whiskers extend from maximum value to minimum value. Line in box is plotted at median.